Journal of Robotics and Control (JRC)
Volume 4, Issue 5, 2023
ISSN: 2715-5072, DOI: 10.18196/jrc.v4i5.18915

Intelligent Hardware-Software Processing of High-Frequency Scanning Data

Zhanna Mukanova [1], Sabyrzhan Atanov [2*], Mohammad Jamshidi [3]
[1] Turan University, Almaty, Kazakhstan,
[2] L.N. Gumilyov Eurasian National University, Astana, Kazakhstan
[3] University of Texas at San Antonio, San Antonio, USA
Email: [1] zhanna.mukanova.83@mail.ru, [2] atanov5@mail.ru, [3] mojamshidi4@gmail.com
*Corresponding Author

***Abstract*—The constant emission of polluting gases is causing an urgent need for timely detection of harmful gas mixtures in the atmosphere. A method and algorithm of the determining spectral composition of gas with a gas analyzer using an artificial neural network (ANN) were suggested in the article. A small closed gas dynamic system was designed and used as an experimental bench for collecting and quantifying gas concentrations for testing the proposed method. This device was based on AS7265x and BMP180 sensors connected in parallel to a 3.3 V compatible Arduino Uno board via QWIIC. Experimental tests were conducted with air from the laboratory room, carbon dioxide (CO_2), and a mixture of pure oxygen (O_2) with nitrogen (N_2) in a 9:1 ratio. Three ANNs with one input, one hidden and one output layer were built. The ANN had 5, 10, and 20 hidden neurons, respectively. The dataset was divided into three parts: 70% for training, 15% for validation, and 15% for testing. The mean square error (MSE) error and regression were analyzed during training. Training, testing, and validation error analysis were performed to find the optimal iteration, and the MSE versus training iteration was plotted. The best indicators of training and construction were shown by the ANN with 5 (five) hidden layers, and 16 iterations are enough to train, test and verify this neural network. To test the obtained neural network, the program code was written in the MATLAB. The proposed scheme of the gas analyzer is operable and has a high accuracy of gas detection with a given error of 3%. The results of the study can be used in the development of an industrial gas analyzer for the detection of harmful gas mixtures.**

***Keywords*—Gas Analyzer; Artificial Neural Network; Harmful Gases; Sensor; Gas Mixture.**

I. INTRODUCTION

Air pollution is one of the current problems in the world, especially in urban areas of developing countries [1]-[3]. With the growth of technological process in the modern world, the number of industrial enterprises increases, the safety level of which, must meet high standards. Timely detection of combustible gases and vapors in the air of industrial premises and territory in concentrations much less than explosive ones and their localization is an important task for compliance with safety rules and fire safety standards [4]-[6].

Gaseous pollutants with characteristics of easily diffuse, difficulty of detection, and harsh treatment have become some of the most harmful pollutants to human health among all industrial wastes [7], [8]. According to the World Health Organization (WHO), in the beginning of August 2023, 91% of the world's population lives in places where air quality exceeds WHO guideline limits, and **7** million people die every year as a result of exposure to fine particles in polluted air [9]. Fig. 1 shows data from the WHO Ambient Air Quality Database for 2012-2022 [10].

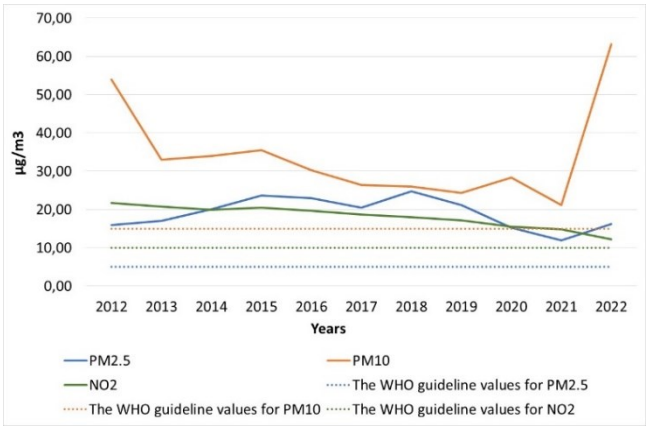

Fig. 1. Ground measurements of annual mean concentrations of nitrogen dioxide (NO_2), particulate matter of a diameter equal or smaller than 10 µm (PM_{10}) or equal or smaller than 2.5 µm ($PM_{2.5}$)

The atmosphere contains many traces of gases such as ozone (O_3), methane (CH_4), carbon monoxide (CO), nitrogen dioxide (NO_2), hydrogen sulfide (H_2S) and sulfur dioxide (SO_2), which exist from a certain concentration and maintain a dynamic equilibrium. Continuous emissions of polluting gases from industry, power generation, as well as car exhaust emissions gradually lead to a decrease in the concentration of gas in the atmospheric environment. As a result, increasingly serious air pollution problems, such as the greenhouse effect and various lung diseases, are occurring [11], [12]. For example, Shwetha, Sharath, Guruprasad, Rudraswamy in [13] state that carbon dioxide (CO_2) has a harmful effect on the ecosystem, causing acid rain, increasing global temperatures and ultimately affecting human health. Therefore, carbon dioxide has traditionally been considered one of the most serious pollutants in the atmosphere. X. Yin and et al. in their paper [14] explain that hydrogen sulfide disrupts the biological process of cell oxidation and prevents cellular respiration, which eventually leads to cell suffocation and hypoxia.

Currently, there is a significant technological growth in the field of artificial intelligence design [15] and, in particular, artificial neural networks [16], [17]. Many new features of neural networks have been discovered in recent

years Works in this field are becoming important contributions to industry, science and technology, and are of great economic importance. For example, in healthcare, ANNs are used to diagnose diseases [18], develop new drugs [19] and treat patients. In finance, ANNs are used to predict the prices of stocks [20], bonds and other financial instruments. In manufacturing, ANNs are used for process optimization, product quality control [21] and logistics management [22]. ANNs have the ability to retrain themselves to improve their performance when new data becomes available.

The use of gas analyzers makes it possible to determine the concentration or type of the analyzed substance in a timely manner by measuring its physical or physical-chemical properties. Using ANN in gas analyzers will allow for the detection of a wider variety of gases. Currently, there are a number of studies on the development of gas analyzers with ANNs. These studies show that ANNs can be used to develop gas analyzers that have higher measurement accuracy than existing gas analyzers, and can also be used to develop gas analyzers that are easier to operate and do not require periodic calibration. Table I summarizes examples of research on the development of gas analyzers of different configurations.

The purpose of this study was to develop a method and algorithm for determining the spectral composition of gas with a gas analyzer using an artificial neural network.

II. Related Work

A neural network (ANN) is a computational model in the form of software and hardware embodiment, inspired by the way that biological neural networks work. A neural network (NN) is a massively parallel processor consisting of elementary units of information processing, learning from experience and applying it to other tasks [28].

The concept of ANNs arose from the study of the processes that occur in the brain and the attempt to model these processes. McCulloch and Pitts [29] were the first scientists to attempt to describe these processes. They demonstrated that the brain consists of a large network of neural units, which act as simple and reliable logical elements. Abiodun, et al. wrote in [30] that ANNs are a model of information management that is similar to the function of the biological nervous system of the human brain.

Artificial neural networks have recently become a popular and useful model for classification, clustering, pattern recognition, and prediction in many disciplines. ANNs are a type of machine learning model, and have become relatively competitive with conventional regression and statistical models in terms of utility [31].

An artificial neural network is a system of connected and interacting simple processors, called artificial neurons. These processors are typically much simpler than the processors used in personal computers. Each processor in the network only deals with the signals it receives and sends to other processors. However, when connected into a large enough network with controlled interaction, these individually simple processors can perform rather complicated tasks [32].

Currently, ANNs are used for prediction [33], [34], pattern recognition [35], [36], machine translation [37], audio recognition [38] and other tasks in various fields of human activity [39]-[41].

For example, Lu, et al. developed an artificial neural network (ANN) and convolutional neural network (CNN) to predict the amorphous forming capacity of various amorphous alloys [42]. Bedford and Hanson investigated the performance of a recurrent neural network for image processing to detect delivery errors during portal dosimetry in volume-modulated arc therapy as early as possible in the treatment process [43]. Sinzinger, Kerkvoorde, Pahr, and Moreno applied spherical CNNs to estimate the apparent stiffness tensor of trabecular bone [44]. Raissi, Perdikaris, and Karniadakis applied physics-based neural networks to solve forward and inverse problems involving nonlinear partial differential equations [45].

III. Methods

A. Development of the Gas Analyzer Circuit

There are several classifications of gas analyzers, which differ in design and functional purpose, and the principle of operation of the sensor elements (sensors). Based on the principle of operation of sensors (sensitive elements, sensors), the authors divide gas analyzers into the following types:

1) Gas analyzers with thermocatalytic (thermochemical) sensors [46];
2) Gas analyzers with thermoconductometric sensors [47];
3) Gas analyzers with infrared sensors (IRS) (also with optical sensors) [48];

TABLE I. Examples of Research on the Development of Gas Analyzers

No.	Sensor type	Number of input signals	Detected gases	AI presence	Error	Accuracy	Reference
1	Semiconductor	6	Ethanol vapors	No AI	3%	-	[23]
2	Resonant photoacoustic	2	Carbon monoxide (CO) and hydrogen sulfide (H_2S)	No AI	-	-	[14]
3	Semiconductor	1	Carbon monoxide (CO) and hydrocarbons (HC)	No AI	-	73,68%	[24]
4	Semiconductor	2	Methane (CH_4) and и carbon monoxide (CO)	Yes, ANN	5%	-	[25]
5	Optical	2	Carbon dioxide (CO_2)	Yes, ANN	-	70,028%	[26]
6	Thermal conductivity	4	Reference gas	Yes, Adaptive Neuro-Fuzzy Inference System (ANFIS)	5%	-	[27]

4) Gas analyzers with semiconductor sensors [49];
5) Gas analyzers with electrochemical sensors [50];
6) Gas analyzers with flame-ionization sensors [51];
7) Flame temperature analyzers [52];
8) Gas analyzers with paramagnetic oxygen sensors [53], [54].

Each type of these gas analyzers has a number of advantages and disadvantages and is used in certain cases. For the present study, gas analyzers with infrared sensors are of the greatest interest.

The principle of operation of optical infrared sensors is based on the absorption of energy from a light beam by the molecules of the gas being detected in the ultraviolet, visible, or infrared region of the spectrum [55]. Existing gas analyzers mainly operate in the infrared region of the spectrum. Infrared sensors do not alter the sample and do not require oxygen to operate. The output signal of infrared sensors is relatively independent of the sample flow rate. They have a long service life and are not susceptible to corrosion, contamination, or mechanical damage. This type of sensor can be used for self-diagnostics to verify the sensitivity to the component being detected. Other advantages of this method include:

a) high stability;
b) no ambiguity of readings at concentrations exceeding the lower concentration limit of flame propagation;
c) resistance to poisoning;
d) less frequent maintenance due to self-diagnostics

Automatic calibration, the ability to monitor the infrared source for proper operation, and the ability to compensate for optical contamination can extend maintenance-free operation. However, special attention should be paid to the timely cleaning of the protective filters in the gas channel, as self-diagnostic tools usually do not detect their contamination. A schematic of the gas analyzer used in this study is shown in Fig. 2.

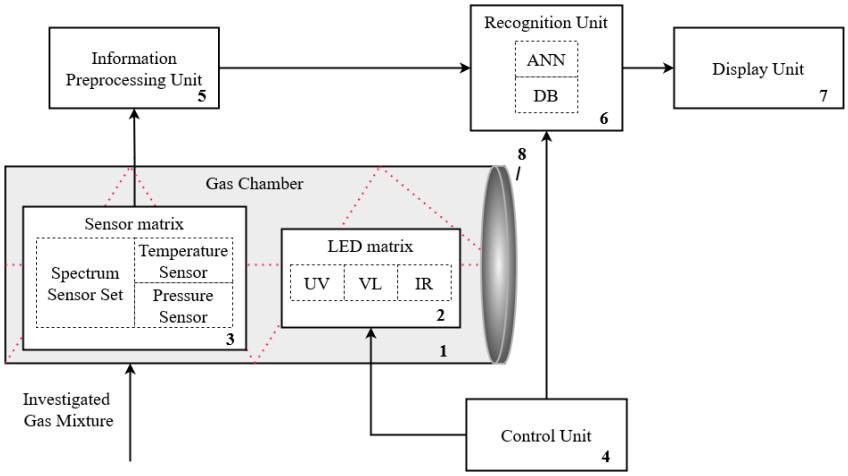

Fig. 2. Schematic diagram of the gas analyzer

The gas analyzer consists of a gas chamber (1), a set of visible, infrared, and ultraviolet radiation sources (2), controlled by the control unit (4), a sensor matrix (3), a preprocessing unit (5), a recognition unit (6), a display unit (7).

In operation, the gas mixture under analysis enters the gas chamber (1) through a parabolic diffuser (8). Pulsed radiation is generated by the corresponding radiation source (matrix of LEDs) (2), controlled by the control unit (4), and enters the chamber (1). The radiation passes through the measuring chamber (1), where part of the radiation energy is absorbed by the gas components, causing the formation of acoustic waves. These waves are detected by the sensor matrix (3), which consists of a set of spectral sensors and temperature and pressure sensors. The electrical signals from the sensors (3) are fed to the input of the preprocessing unit (5). The preprocessing unit (5) extracts several hundred parameters of the gas mixture. The signal with the results of calculating the parameters of the gas mixture from the preprocessing unit (5) is fed to the input of the recognition unit (6), which consists of a trained neural network and a database of gas mixtures. The trained neural network, interacting with the database of gas mixtures, outputs a state "1" on one of its outputs, and this state is displayed by the display unit (7).

If a beam of radiation interrupted at a certain frequency is directed into a vessel containing a gas that can absorb infrared radiation, then a pressure pulsation will occur in the gas, which is subjectively perceived as sound. The pressure pulsation occurs because the gas molecules, absorbing photons of incident radiation, go to an excited state, and then the excitation energy of their vibrational-rotational degrees of freedom is transferred, as a result of inelastic collisions between molecules, into the translational motion energy of the latter, i.e. into heat, which corresponds to an increase in pressure. The use of a parabolic emitter (8) in this design will provide multiple passages of the rays through the chamber (3), thereby increasing the gas pressure in the chamber.

B. Development of a Prototype Gas Analyzer for Data Collection

There are a large number of different sensors available for making measurements [56], [57]. Sensors are widely used in various fields, such as scientific research, testing, quality control, automated control systems, and others [58]-[60]. As part of the development of a prototype gas analyzer designed to determine the concentration of multicomponent gas mixtures in air in laboratory and industrial conditions, the AS7265x and BMP180 sensors were used.

The SparkFun Triad spectroscopic sensor is a powerful optical control sensor, also known as a spectrophotometer [61]. Three AS7265x spectral sensors are combined with UV and IR LEDs to illuminate and test various surfaces for light spectroscopy. The triad consists of three sensors: the AS72651, AS72652, and AS72653, which can detect light from 410 nm (UV) to 940 nm (IR) (Fig. 3). Each sensor has six independent see optical filters. There are a total of 18 output channels. The use of spectral sensors combined with ultraviolet and infrared LEDs greatly simplifies the design of the gas analyzer and increases the measurement accuracy [62].

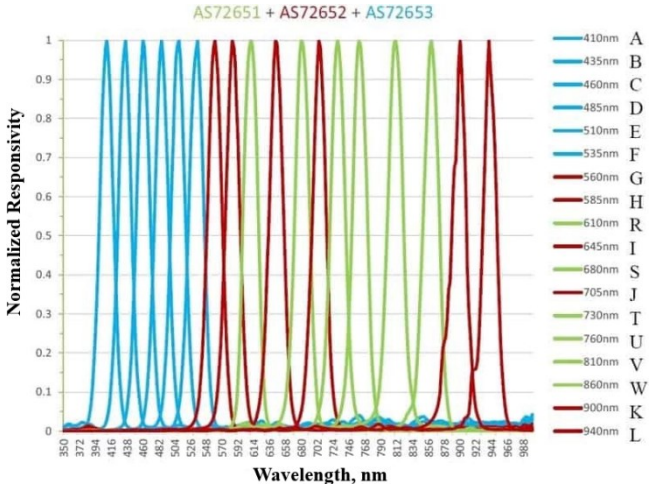

Fig. 3. 18 Chanel spectral respons

The BMP180 sensor can be used to measure absolute atmospheric pressure in the range of 300 to 1100 hPa (+9000 to -500 meters above sea level) [63]. It can be used in home weather stations, flying vehicles, as an altimeter, and other applications. The GY-68 module, which is based on the BMP180 chip, combines an atmospheric pressure sensor and a thermometer.

Fig. 4 shows a multispectral sensor system with artificial intelligence (AI) support. The AS7265x and BMP180 sensors are connected in parallel to a 3.3 V compatible Arduino Uno [64] board using a QWIIC cable. The Arduino board is used as a microcontroller to receive and transmit digitized sensor signal data to a laptop computer via the USB port. The received spectral data are stored for preprocessing [65]. The preprocessed sample data is transferred to a non-linear neural network for further analysis. These preprocessed data are used to train, test, and validate the neural network [66].

Fig. 5 shows a block diagram of the gas analyzer operation. To create the tested devices, an experimental bench was built. It is a small, closed gas dynamic system for collecting and quantitatively determining the gas concentration using sensors. The system consists of the following main components: an Arduino microprocessor board, AS7265x and BMP180 sensors, a container for circulating the analyzed gas mixture, a container for generating gas, a power supply unit and a circulation pump (Fig. 7).

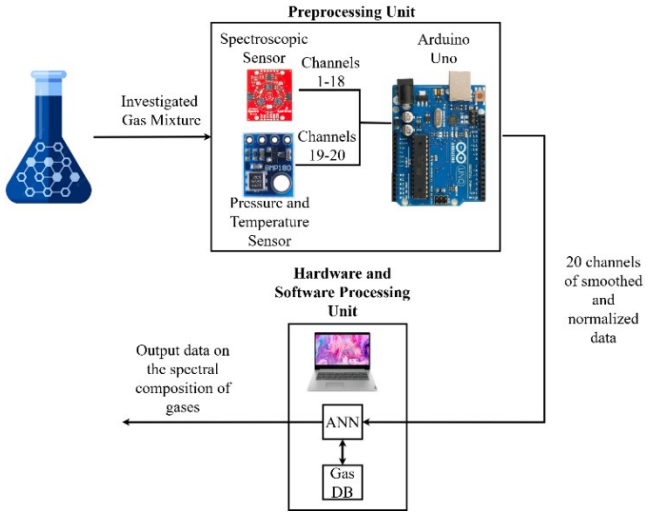

Fig. 4. Multispectral sensor system with Artificial Intelligence (AI) support

Fig. 5. General view of the laboratory bench for gas collection and analysis

C. Data Collection and Preprocessing

The spectral data collected from the Arduino module is transferred to a PC via the USB port. The data is then formatted in a form that machine learning algorithms can accept using the MS Excel spreadsheet editor. Outliers, duplicate data, and redundant data beyond the standard size were also removed [67].

D. Neural Network Model

The pre-processed spectral data is fed as input to the neural network architecture. Fig. 6 shows the neural network architecture, which has 20 input layers, followed by hidden layers, and a multilayer output for multiclassification.

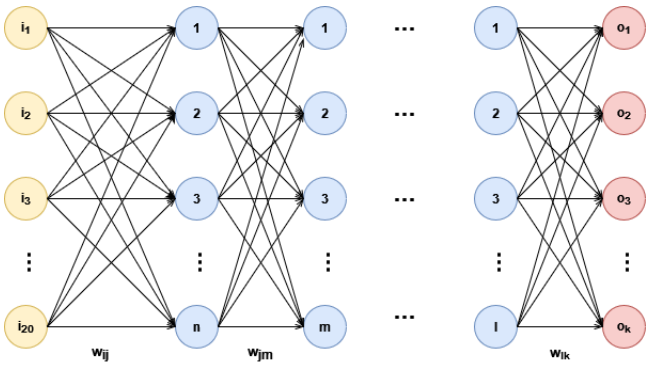

Fig. 6. Neural network architecture

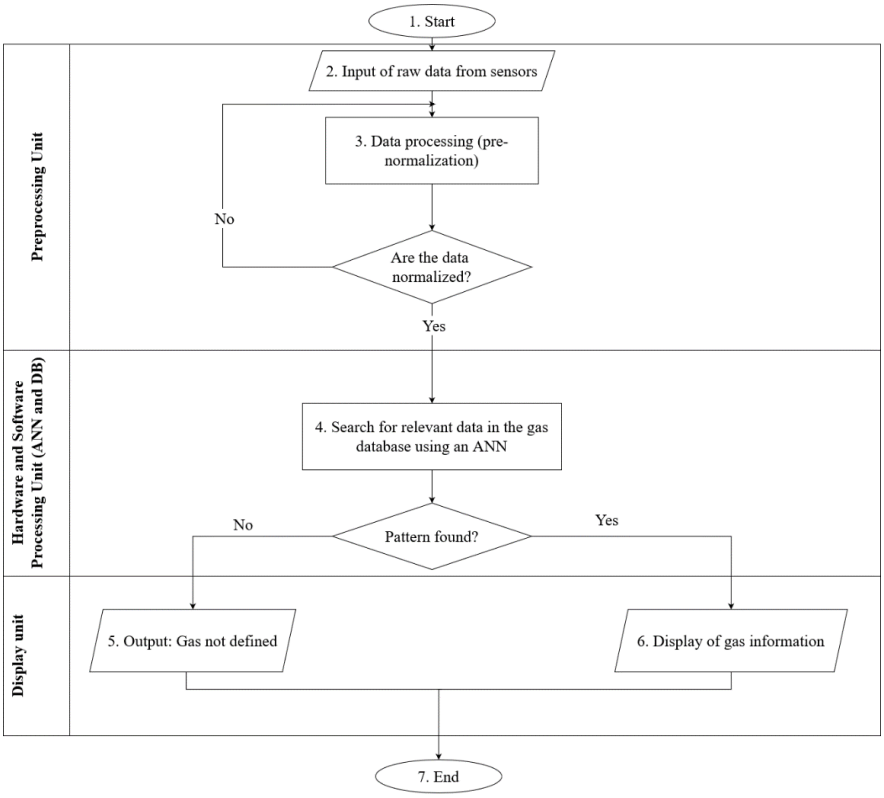

Fig. 7. Block diagram of the gas analyzer

From Fig. 6, the preprocessed spectral data fed to the input layer has 20 inputs, since our circuit has 20 channels with different wavelengths. In this network layout, i_1, i_2, ..., i_{20} represent the input neurons, w_{ij} represent the weights connecting the input to the hidden layer, w_{jm} represent the weights present in the interconnected hidden layers, and w_{lk} represent the weights connecting the hidden layer to the output layer.

Training of the neural network is performed using the backpropagation of error method [68], [69]. In the training process, the weights are adjusted so that a set of inputs leads to the required set of outputs. It is initially assumed that each input set corresponds to its paired target set, which specifies the required output. Together, they form a training pair [70], [71].

Initially, the weights and offsets are assigned randomly and processed together with the input data using the forward propagation method. The output error value is calculated by comparing the actual value and the predicted value. The output error is then minimized using a gradient descent algorithm. The cross-entropy is used as a loss function [72].

To constrain the search space during training, the task is to minimize the NS target error function, which is found using the least squares method [73] as shown in (1).

$$E(w) = \frac{1}{2}\sum_{j=1}^{p}(y_j - d_j)^2 \quad (1)$$

Where, y_j is the value of the j-th output of the neural network; d_j is the target value of the j-th output; p is the number of neurons in the output layer.

The combination of the least squares method with the gradient descent method is called the Levenberg–Marquardt algorithm [74]. The block diagram of the backpropagation of error method algorithm is shown in Fig. 8.

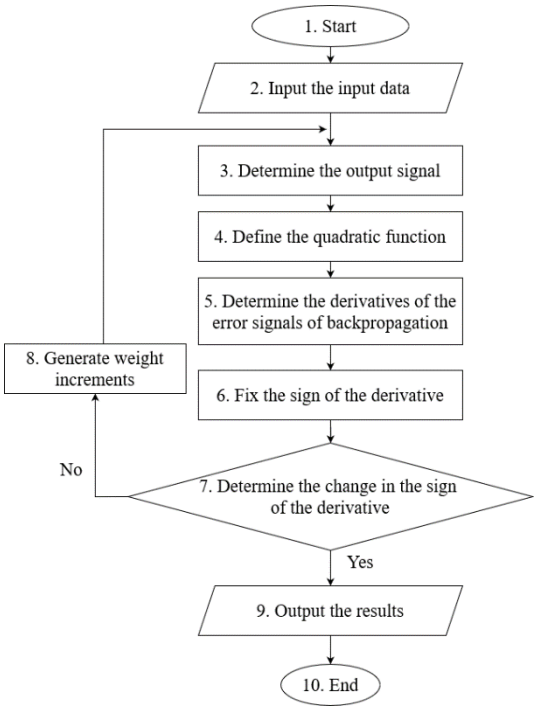

Fig. 8. Block diagram of the error backpropagation algorithm

The Neural Network Start (NNStart) package of MATLAB [75], [76] was used to implement ANN training. The NNStart package allows for curve approximation, image recognition, object clustering, and time series approximation.

IV. RESULTS

For experimental tests of the laboratory bench (Fig. 6), a sample of air from the laboratory room, carbon dioxide (CO_2), and a mixture consisting of pure oxygen (O_2) with nitrogen (N_2) in a 9:1 ratio were fed in turn into the container for circulation of the analyzed gas mixture. The experiments were performed in a well-ventilated room of 20 m^2.

Using the NNStart package, a neural network (NS) with one input, one hidden, and one output layer was designed. The neurons on the hidden layer have a sigmoidal activation function [77], and those on the output layer have a linear function [78].

At the initial stage of an neural network design, the volume of training, validation, and test samples is determined. The training sample is used to train the ANN. The test sample is used to evaluate the generalization properties of the network, and to stop training when the generalization stops improving. The test sample has no effect on training, but serves to test the quality of training on data that was not used in training the network. The more sample volume is, the more accurate results the neural network will produce.

Two types of analysis were performed to determine the number of neurons in the hidden layer. The first consisted in revealing the dependence of the training time on the number of neurons (Fig. 9).

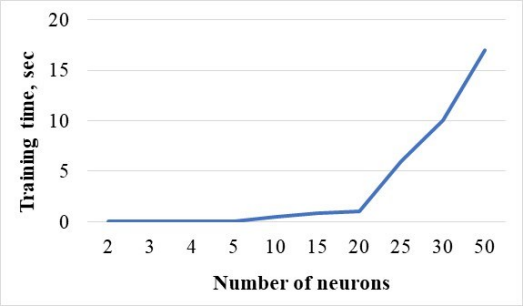

Fig. 9. Dependence of NN training time on the number of neurons in the hidden layer

As can be seen from the graph, the training time of the neural network increases sharply when the number of neurons is more than 20. The second analysis showed how the number of neurons affects the magnitude of the gradient of the error function (Fig. 10).

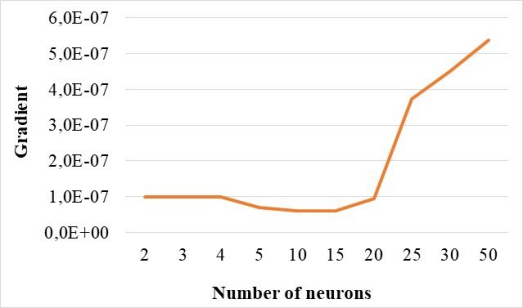

Fig. 10. Dependence of the gradient of the neural network error function on the number of neurons in the hidden layer

As can be seen from the graph, the gradient of the training error sharply increases in the range of 20 to 50 neurons. This indicates the appearance of overfitting. In such cases, it is usually recommended to reduce the number of hidden elements and/or layers, because the network is too powerful for the task. The most favorable situation is when the training error decreases. On the graph, this situation is observed in the range of 4 to 15 layers.

After analyzing both graphs, it was decided to build three neural networks with 5, 10, and 20 neurons and compare the results.

A) A Neural Network Model with Five Neurons in a Hidden Layer

The spectral data samples were organized such that 70% of the data set was used for training, 15% was used for validation, and the remaining 15% was used for testing. The training data was used to train the network, and the network was also tuned according to the error. The validation sample was used to evaluate the performance of the network and to stop training when the network was no longer improving. The test samples were used to measure the accuracy of the network on unseen data. The results of training are shown in Table II. In Table III shows the number of observations, root mean square error (MSE), and R-squared during training.

TABLE II. NEURAL NETWORK TRAINING RESULTS

Unit	Initial Value	Stopped Value	Target Value
Epoch	0	16	1000
Elapsed Time	-	00:00:00	-
Performance	2.12	1.39e-15	0
Gradient	3.92	6.9e-08	1e-07
Mu	0.001	1e-15	1e+10
Validation Checks	0	0	0

TABLE III. LEARNING OUTCOMES

Stage	Number of Observations	MSE	R-squared
Training	52	1.3872e-15	1.0000
Validation	11	1.2682e-15	1.0000
Test	11	4.0661e-15	1.0000

Training, testing, and validation error analyses are performed to find the optimal number of epochs. The gradient, cross-entropy, and validation loss during neural network training are shown in Fig. 11.

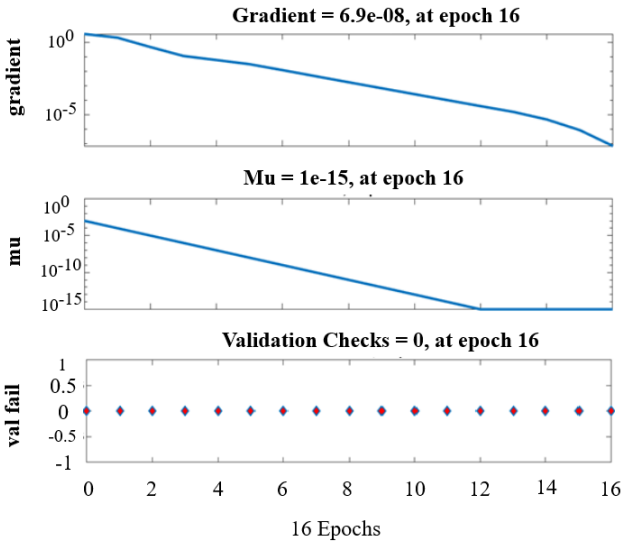

Fig. 11. Results of the training process

Fig. 12 shows a graph of the relationship between the root mean square error (MSE) and the training epoch. The variations of the error for three data sets are shown: training, validation, and test. We can see that the error decreases significantly by the end of the training process.

The best validation accuracy is achieved at epoch 16. The error rate is minimized and reaches zero at epoch 16 during validation. This may be a function of the loss to train the model. The cross-entropy loss decreases as the number of iterations increases, which means that the model learns very well from the data. It minimizes the distance between the predicted value and the actual sample value. From the entire error analysis, we can conclude that the model requires only 16 epochs to train and set the optimal weight value.

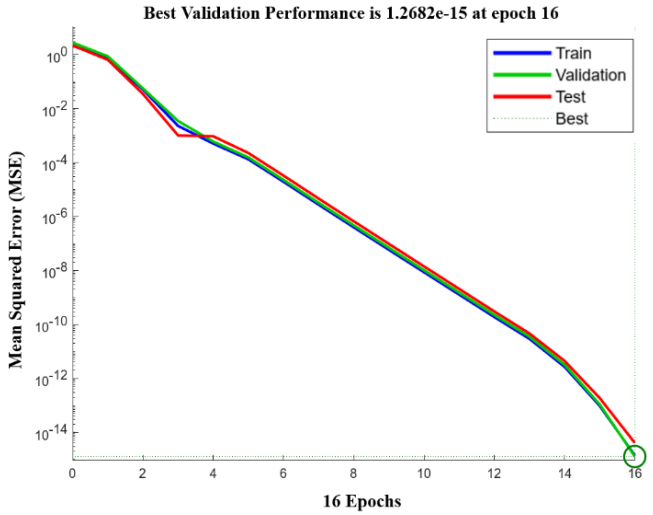

Fig. 12. Variation of network error during the training process

The error histogram provides an additional check on network performance. The blue bars represent training data, the green bars represent validation data, and the red bars represent testing data. The histogram can give you an idea of outliers, that is, data points that match significantly worse than most data. As you can see in Fig. 13, the model is well-optimized at the expense of less error.

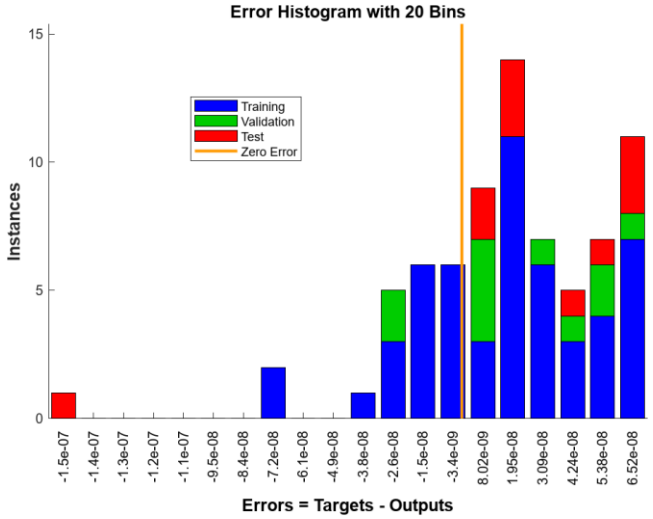

Fig. 13. Error histogram

An additional tool for evaluating the ANN training results is to build regression functions from the ANN output values (Output) to the target values that have been set in the training sample. Fig. 14 shows a linear regression between the ANN output and the targets for the training, validation, and testing datasets.

For a perfect match, the data must lie along a line at a 45-degree angle where the network output is equal to the target values. As you can see in Fig. 14, the perfect match for all datasets has an R value of 1.

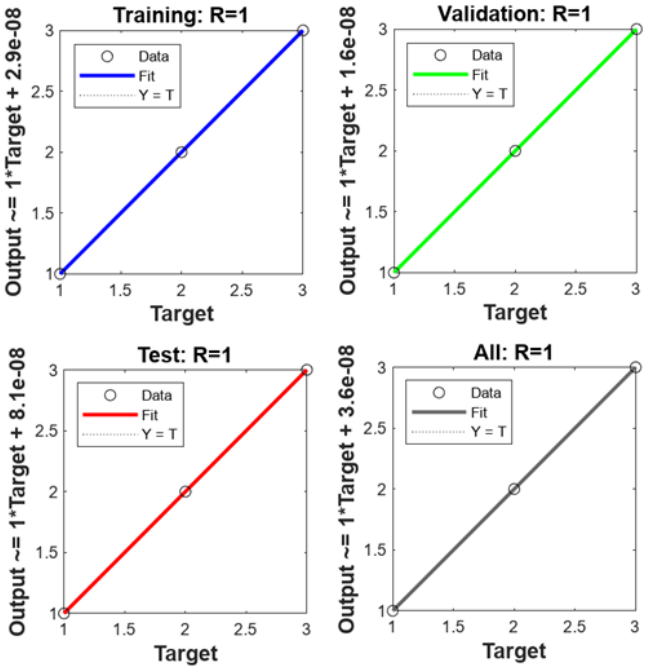

Fig. 14. Linear regression of neural network output and targets

B) A Neural Network Model with Ten Neurons in a Hidden Layer

Sample division parameters: training -70%, validating -15%, testing: 15%. The number of hidden neurons is 10. The results of training are shown in Table IV. In Table V shows the number of observations, root mean square error (MSE), and R-squared during training. Fig. 15 shows the gradient, cross-entropy, and failure rate during neural network training.

TABLE IV. NEURAL NETWORK TRAINING RESULTS

Unit	Initial Value	Stopped Value	Target Value
Epoch	0	19	1000
Elapsed Time	-	00:00:00	-
Performance	2.92	3.26e-16	0
Gradient	6.68	6.03e-08	1e-07
Mu	0.001	1e-15	1e+10
Validation Checks	0	0	0

TABLE V. LEARNING OUTCOMES

Stage	Number of Observations	MSE	R-squared
Training	52	3.2631e-16	1.0000
Validation	11	2.1441e-07	1.0000
Test	11	6.3369e-08	1.0000

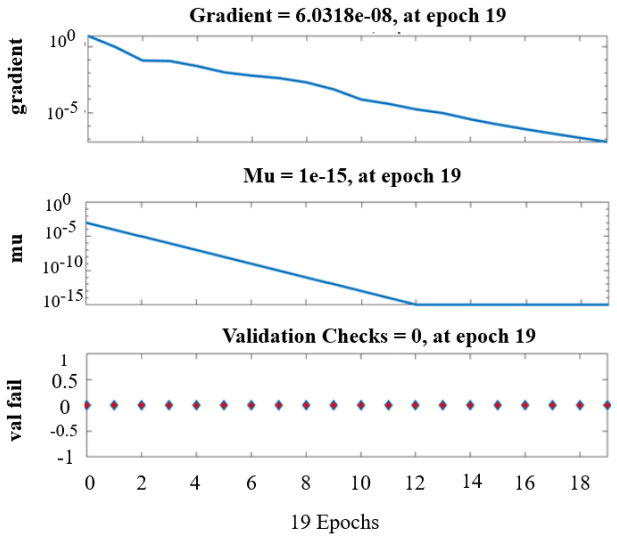

Fig. 15. Results of the training process

Fig. 16 shows a plot of the root mean squared error (MSE) as a function of training epochs. From the error analysis, we can conclude that the model requires 19 epochs to train and set the optimal weight value. As you can see in Fig. 17, the model is well-optimized because the error value is lower.

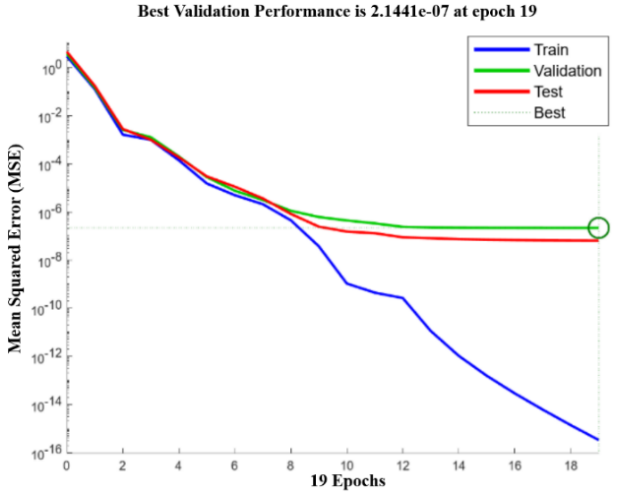

Fig. 16. Variation of network error during the training process

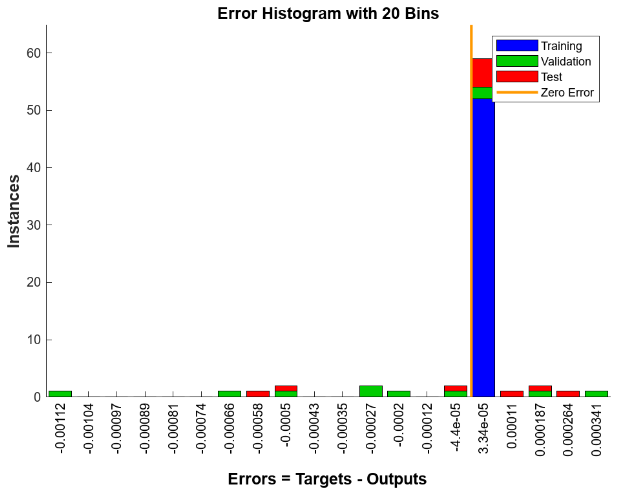

Fig. 17. Error histogram

Fig. 18 shows a linear regression of the neural network's output and targets for the training, validation, and testing datasets.

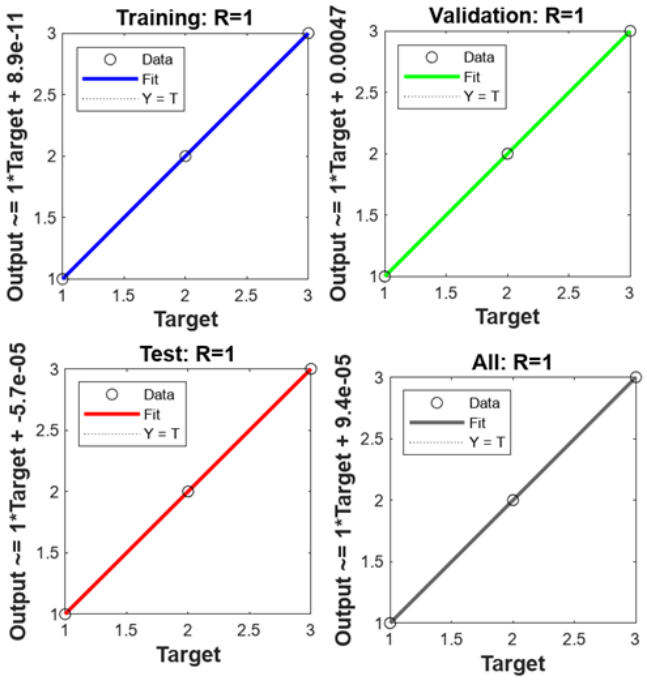

Fig. 18. Linear regression of neural network output and targets

C) A Neural Network Model with Twenty Neurons in a Hidden Layer

Sample division parameters: training -70%, validating -15%, testing: 15%. The number of hidden neurons is 20. The results of training are shown in Table VI. In Table VII shows the number of observations, root mean square error (MSE), and R-squared during training.

TABLE VI. NEURAL NETWORK TRAINING RESULTS

Unit	Initial Value	Stopped Value	Target Value
Epoch	0	50	1000
Elapsed Time	-	00:00:01	-
Performance	6.06	1.08e-12	0
Gradient	18.3	9.4e-08	1e-07
Mu	0.001	1e-08	1e+10
Validation Checks	0	0	0

TABLE VII. LEARNING OUTCOMES

Stage	Number of Observations	MSE	R-squared
Training	52	1.0777e-12	1.0000
Validation	11	0.0043	0.9971
Test	11	0.0062	0.9951

Fig. 19 shows the gradient, cross-entropy, and failure rate during neural network training. Fig. 20 shows a graph of the root mean squared error (MSE) as a function of training epochs. From the error analysis, it can be concluded that the model requires only 50 epochs to train and set the optimal weight value, which is significantly more than in the two previous neural network variants. As you can see in Fig. 21, the model is well-optimized because the error value is lower.

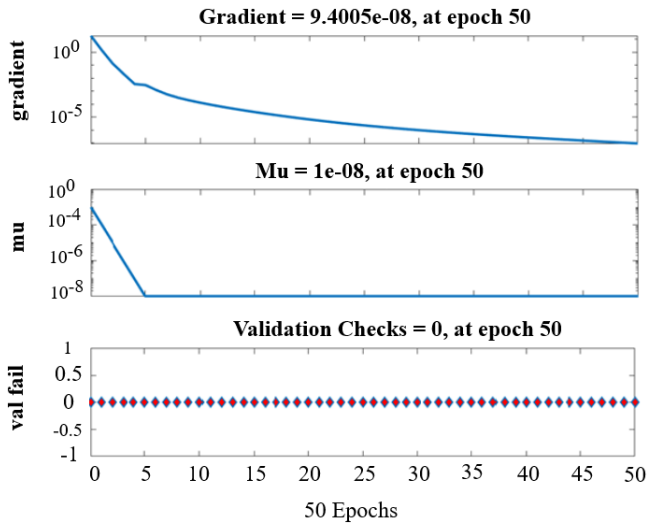

Fig. 19. Results of the training process

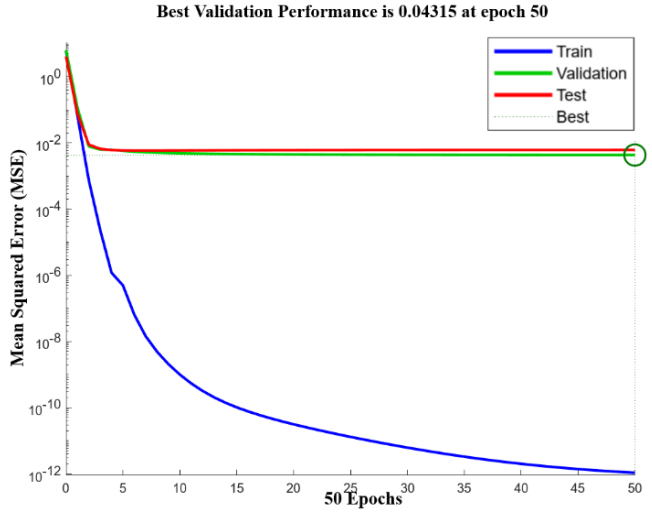

Fig. 20. Variation of network error during the training process

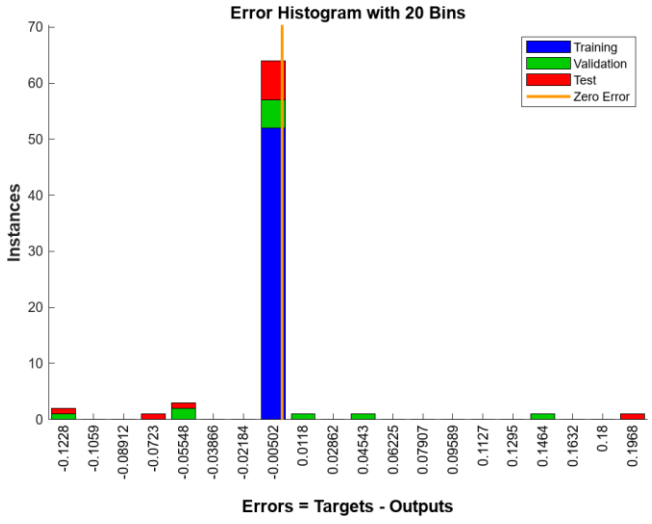

Fig. 21. Error histogram

Fig. 22 shows a linear regression of the neural network's output and targets for the training, validation, and testing datasets.

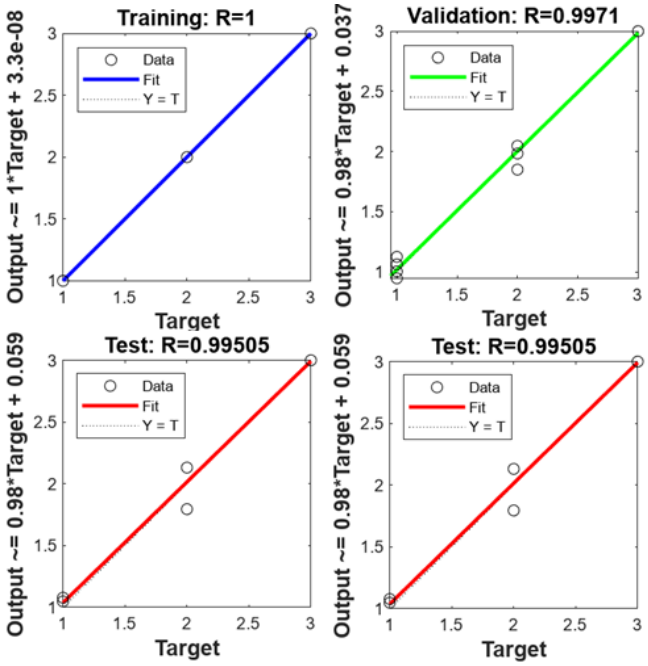

Fig. 22. Linear regression of neural network output and targets

D) Approval of the Neural Network Model

To test the neural network, we wrote a program in MATLAB. In turn, we fed a sample of laboratory air, carbon dioxide (CO2), and a mixture of pure oxygen (O2) and nitrogen (N2) in a 9:1 ratio into the circulation container for the analyzed gas mixture of the assembled laboratory bench. The sensor data from the assembled laboratory bench was fed sequentially into the program input. After additional preparation, the data was transferred to the input of each of the neural networks. The program output was a visualization of the gas mixture. Fig. 23 shows the output window of the program. The program results show that there are gases unknown to the database.

Command Window

NN5	NN10	NN20
O2+N2	O2+N2	O2+N2
O2+N2	O2+N2	O2+N2
O2+N2	O2+N2	O2+N2
Unknown	O2+N2	O2+N2
O2+N2	O2+N2	O2+N2
O2+N2	O2+N2	O2+N2
O2+N2	O2+N2	O2+N2
CO2	CO2	CO2
CO2	Unknown	CO2
CO2	Unknown	CO2
CO2	CO2	CO2
CO2	CO2	CO2
CO2	CO2	CO2
CO2	CO2	CO2
Empty	Empty	Empty
Empty	Empty	Empty
Empty	Empty	Empty
Empty	Empty	Empty

Fig. 23. Program results

V. CONCLUSIONS

The aim of this study was to develop a method and algorithm for determining the spectral composition of gas. Advanced spectroscopic methods and sensors were used, including sensors that allow obtaining data in the UV and IR range. Gas pressure and temperature data were also used to increase the accuracy of the analysis and the measurement range of the input data. Neural networks were used to analyze the spectral composition of gas mixtures with high accuracy, even in the presence of unknown gases.

An experimental bench was built to test this concept. It is a small, closed gas dynamic system for collecting and quantifying gas concentrations using sensors. The system consists of the following main components: Arduino microprocessor board, AS7265x and BMP180 sensors, container for circulating the analyzed gas mixture, container for generating gas, power supply unit, circulation pump.

A sample of laboratory air, carbon dioxide (CO_2), and a mixture consisting of pure oxygen (O_2) and nitrogen (N_2) in a 9:1 ratio were fed into the circulation container for the analyzed gas mixture in turn.

Three neural networks were constructed using the NNStart package of the MATLAB mathematical system. Each neural network has one input layer, one hidden layer, and one output layer. The neural networks differed in the way they sampled spectral data, namely the number of hidden neurons.

Training and construction of each of the obtained neural networks showed good results. However, the graph of the network error variation in the process of training for a neural network with five hidden layers is the most successful and demonstrative. The MSE of training, verification, and test results for a neural network with five hidden layers are also the most optimal.

The results of this study prove that the proposed gas analyzer scheme is functional, and the software created provides an effective analysis of the composition of gas mixtures. Experimental studies have shown a high accuracy of gas detection for this type of device with a given error of 3% of gas detection A neural network with five hidden layers and 16 iterations is sufficient for this purpose.

The proposed gas analyzer scheme is based on the model described in the patent «Gas analyzer» No. 5141 dated 10.07.2020 [79], which was further developed in the patent «Intelligent gas analyzer» No. 8288 dated 21.03.2023 [80], using neural networks for decision analysis.

In the future, it is planned to implement an autonomous gas analyzer based on Raspberry Pi or Arduino Mega microcontrollers. This will make the device more compact and portable, and the use of a trained database will allow the proposed method to be effectively implemented on FPGAs. All this will make it more convenient and autonomous for use in the field. It is also planned to test this concept using convolutional neural networks, which will simplify calculations while maintaining accuracy. This will allow to increase the speed of data processing, conduct data analysis in real time and obtain more accurate results. These improvements will make the device more reliable and durable. This will allow it to be used in industrial conditions.

ACKNOWLEDGEMENTS

The researchers would like to thank the Science Committee of the Ministry of Science and Higher Education of the Republic of Kazakhstan for funding this research through grant (Program No. AP19677508).

REFERENCES

[1] J. da Motta Singer *et al*., "Assessing socioeconomic bias of exposure to urban air pollution: an autopsy-based study in São Paulo, Brazil," *The Lancet Regional Health - Americas*, vol. 22, p. 100500, 2023, doi: 10.1016/j.lana.2023.100500.

[2] J. Badach, W. Wojnowski, and J. Gębicki, "Spatial aspects of urban air quality management: Estimating the impact of micro-scale urban form on pollution dispersion," *Computers, Environment and Urban Systems*, vol. 99, p. 101890, 2023, doi: 10.1016/j.compenvurbsys.2022.101890.

[3] P. Hystad, S. Yusuf, and M. Brauer, "Air pollution health impacts: the knowns and unknowns for reliable global burden calculations," *Cardiovascular Research*, vol. 116, no. 11, pp. 1794–1796, 2020, doi: 10.1093/cvr/cvaa092.

[4] A. Bayramova, D. J. Edwards, C. Roberts, and I. Rillie, "Enhanced safety in complex socio-technical systems via safety-in-cohesion," *Safety Science*, vol. 164, p. 106176, 2023, doi: 10.1016/j.ssci.2023.106176.

[5] R. Dârmon, "Probabilistic Methods to Assess the Fire Risk of an Industrial Building," *Procedia Manufacturing*, vol. 46, pp. 543–548, 2020, doi: 10.1016/j.promfg.2020.03.078.

[6] M. A. Ibrahim, A. Lönnermark, and W. Hogland, "Safety at waste and recycling industry: Detection and mitigation of waste fire accidents," *Waste Management*, vol. 141, pp. 271–281, 2022, doi: 10.1016/j.wasman.2022.02.004.

[7] S. Zheng *et al*., "Effects of short-term exposure to gaseous pollutants on metabolic health indicators of patients with metabolic syndrome in Northwest China," *Ecotoxicology and Environmental Safety*, vol. 249, p. 114438, 2023, doi: 10.1016/j.ecoenv.2022.114438.

[8] H. S. Iyer *et al*., "Impacts of long-term ambient particulate matter and gaseous pollutants on circulating biomarkers of inflammation in male and female health professionals," *Environmental Research*, vol. 214, p. 113810, 2022, doi: 10.1016/j.envres.2022.113810.

[9] L. M. G. Peláez, J. M. Santos, T. T. de Almeida Albuquerque, N. C. Reis Jr, W. L. Andreão, and M. de Fátima Andrade, "Air quality status and trends over large cities in South America," *Environmental Science & Policy*, vol. 114, pp. 422-435, 2020.

[10] World Health Organization. *WHO ambient air quality database, 2022 update: status report*. World Health Organization, 2023.

[11] P. Lott and O. Deutschmann, "Heterogeneous chemical reactions—A cornerstone in emission reduction of local pollutants and greenhouse gases," *Proceedings of the Combustion Institute*, vol. 39, no. 3, pp. 3183–3215, 2023, doi: 10.1016/j.proci.2022.06.001.

[12] S. Harari, G. Raghu, A. Caminati, M. Cruciani, M. Franchini, and P. Mannucci, "Fibrotic interstitial lung diseases and air pollution: a systematic literature review," *European Respiratory Review*, vol. 29, no. 157, p. 200093, 2020, doi: 10.1183/16000617.0093-2020.

[13] H. R. Shwetha, S. M. Sharath, B. Guruprasad, and S. B. Rudraswamy, "MEMS based metal oxide semiconductor carbon dioxide gas sensor," *Micro and Nano Engineering*, vol. 16, p. 100156, 2022, doi: 10.1016/j.mne.2022.100156.

[14] X. Yin *et al*., "Near-infrared laser photoacoustic gas sensor for simultaneous detection of CO and H2S," *Optics Express*, vol. 29, no. 21, p. 34258, 2021, doi: 10.1364/oe.441698.

[15] I. Ahmed, G. Jeon, and F. Piccialli, "From Artificial Intelligence to Explainable Artificial Intelligence in Industry 4.0: A Survey on What, How, and Where," *IEEE Transactions on Industrial Informatics*, vol. 18, no. 8, pp. 5031–5042, 2022, doi: 10.1109/tii.2022.3146552.

[16] B. Kim, S. Lee, and J. Kim, "Inverse design of porous materials using artificial neural networks," *Science Advances*, vol. 6, no. 1, 2020, doi: 10.1126/sciadv.aax9324.

[17] P. G. Asteris and V. G. Mokos, "Concrete compressive strength using artificial neural networks," *Neural Computing and Applications*, vol. 32, no. 15, pp. 11807–11826, 2019, doi: 10.1007/s00521-019-04663-2.

[18] D. A. Gavrilov, A. V. Melerzanov, N. N. Shchelkunov, and E. I. Zakirov, "Use of Neural Network-Based Deep Learning Techniques for the Diagnostics of Skin Diseases," *Biomedical Engineering*, vol. 52, no. 5, pp. 348–352, 2019, doi: 10.1007/s10527-019-09845-9.

[19] K.-K. Mak and M. R. Pichika, "Artificial intelligence in drug development: present status and future prospects," *Drug Discovery Today*, vol. 24, no. 3, pp. 773–780, 2019, doi: 10.1016/j.drudis.2018.11.014.

[20] K. C. S, "Hybrid models for intraday stock price forecasting based on artificial neural networks and metaheuristic algorithms," *Pattern Recognition Letters*, vol. 147, pp. 124–133, 2021, doi: 10.1016/j.patrec.2021.03.030.

[21] M. Malesa and P. Rajkiewicz, "Quality Control of PET Bottles Caps with Dedicated Image Calibration and Deep Neural Networks," *Sensors*, vol. 21, no. 2, p. 501, 2021, doi: 10.3390/s21020501.

[22] Q. Liang, "Production Logistics Management of Industrial Enterprises Based on Wavelet Neural Network," *Journal Européen des Systèmes Automatisés*, vol. 53, no. 4, pp. 581–588, 2020, doi: 10.18280/jesa.530418.

[23] P. W. Alexander, L. T. Di Benedetto, and D. B. Hibbert, "A field-portable gas analyzer with an array of six semiconductor sensors. Part 1: Quantitative determination of ethanol," *Field Analytical Chemistry & Technology*, vol. 2, no. 3, pp. 135–143, 1998.

[24] M. Khatami, A. Sujatmiko, and A. Asrori, "An Analysis of Emission Exhaust Gas on 4-Stroke Engine Based on IOT Gas Analyzer," *Logic: Jurnal Rancang Bangun Dan Teknologi*, vol. 23, no. 2, pp. 104–110, 2023.

[25] A. M. Trunin, A. N. Ragozin, and S. N. Darovskih, "An Investigation of the Application of an Artificial Neural Network and Machine Learning to Improve the Efficiency of Gas Analyzer Systems in Assessing the State of the Environment," *2021 International Conference on Industrial Engineering, Applications and Manufacturing (ICIEAM)*, pp. 571-575, 2021, doi: 10.1109/ICIEAM51226.2021.9446406.

[26] G. Zhang and X. Wu, "A novel CO2 gas analyzer based on IR absorption," *Optics and Lasers in Engineering*, vol. 42, no. 2, pp. 219–231, 2004, doi: 10.1016/j.optlaseng.2003.08.001.

[27] J. L. G. Medialdea, M. E. C. Manamparan, M. G. M. Sorita, E. L. Ponce, and A. A. Beltran Jr., "A novel thermal gas analyzer using adaptive neuro-fuzzy inference system (ANFIS)," *Institute of Electronics Engineers of the Philippines (IECEP) Journal*, vol. 2, no. 1, pp. 27–31, 2013.

[28] F. A. Ghani, M. Rivaie, M. Yusoff, and M. Puteh, "A Review of Artificial Neural Network Applications in Variants of Optimization Algorithms," *2022 International Visualization, Informatics and Technology Conference (IVIT)*, pp. 115-123, 2022, doi: 10.1109/IVIT55443.2022.10033339.

[29] G. Piccinini, "The First Computational Theory of Cognition," *Neurocognitive Mechanisms: Explaining Biological Cognition*, pp. 107–127, 2020, doi: 10.1093/oso/9780198866282.003.0006.

[30] O. I. Abiodun, A. Jantan, A. E. Omolara, K. V. Dada, N. A. Mohamed, and H. Arshad, "State-of-the-art in artificial neural network applications: A survey," *Heliyon*, vol. 4, no. 11, p. e00938, 2018, doi: 10.1016/j.heliyon.2018.e00938.

[31] M. G. M. Abdolrasol *et al*., "Artificial Neural Networks Based Optimization Techniques: A Review," *Electronics*, vol. 10, no. 21, p. 2689, 2021, doi: 10.3390/electronics10212689.

[32] S. Bai, G. Fang, and J. Zhou, "Construction of three-dimensional extrusion limit diagram for magnesium alloy using artificial neural network and its validation," *Journal of Materials Processing Technology*, vol. 275, p. 116361, 2020, doi: 10.1016/j.jmatprotec.2019.116361.

[33] N. Lamii, M. Fri, C. Mabrouki, and E. A. Semma, "Using Artificial Neural Network Model for Berth Congestion Risk Prediction," *IFAC-PapersOnLine*, vol. 55, no. 12, pp. 592–597, 2022, doi: 10.1016/j.ifacol.2022.07.376.

[34] A. Bouteska, P. Hajek, B. Fisher, and M. Z. Abedin, "Nonlinearity in forecasting energy commodity prices: Evidence from a focused time-delayed neural network," *Research in International Business and Finance*, vol. 64, p. 101863, 2023, doi: 10.1016/j.ribaf.2022.101863.

[35] A. Wang, W. Zhang, and X. Wei, "A review on weed detection using ground-based machine vision and image processing techniques," *Computers and Electronics in Agriculture*, vol. 158, pp. 226–240, 2019, doi: 10.1016/j.compag.2019.02.005.

[36] M. Mirbod and M. Shoar, "Intelligent Concrete Surface Cracks Detection using Computer Vision, Pattern Recognition, and Artificial Neural Networks," *Procedia Computer Science*, vol. 217, pp. 52–61, 2023, doi: 10.1016/j.procs.2022.12.201.

[37] S. K. Sheshadri, D. Gupta, and M. R. Costa-Jussà, "A Voyage on Neural Machine Translation for Indic Languages," *Procedia Computer Science*, vol. 218, pp. 2694–2712, 2023, doi: 10.1016/j.procs.2023.01.242.

[38] L. Tessarini and A. M. F. Fileti, "Audio signals and artificial neural networks for classification of plastic resins for recycling," *Digital Chemical Engineering*, vol. 5, p. 100059, 2022, doi: 10.1016/j.dche.2022.100059.

[39] V. Balaji *et al*., "Deep Transfer Learning Technique for Multimodal Disease Classification in Plant Images," *Contrast Media & Molecular Imaging*, vol. 2023, pp. 1–8, 2023, doi: 10.1155/2023/5644727.

[40] X. Liu, S. Xiong, X. Wang, T. Liang, H. Wang, and X. Liu, "A compact multi-branch 1D convolutional neural network for EEG-based motor imagery classification," *Biomedical Signal Processing and Control*, vol. 81, p. 104456, 2023, doi: 10.1016/j.bspc.2022.104456.

[41] A. Abdalla *et al*., "Fine-tuning convolutional neural network with transfer learning for semantic segmentation of ground-level oilseed rape images in a field with high weed pressure," *Computers and Electronics in Agriculture*, vol. 167, p. 105091, 2019, doi: 10.1016/j.compag.2019.105091.

[42] F. Lu *et al*., "Prediction of amorphous forming ability based on artificial neural network and convolutional neural network," *Computational Materials Science*, vol. 210, p. 111464, Jul. 2022, doi: 10.1016/j.commatsci.2022.111464.

[43] I. Hanson and J. Bedford, "A recurrent neural network for identifying delivery errors during real-time portal dosimetry," *Physica Medica*, vol. 104, pp. S156–S157, 2022, doi: 10.1016/s1120-1797(22)02493-0.

[44] F. Sinzinger, J. van Kerkvoorde, D. H. Pahr, and R. Moreno, "Predicting the trabecular bone apparent stiffness tensor with spherical convolutional neural networks," *Bone Reports*, vol. 16, p. 101179, 2022, doi: 10.1016/j.bonr.2022.101179.

[45] M. Raissi, P. Perdikaris, and G. E. Karniadakis, "Physics-informed neural networks: A deep learning framework for solving forward and inverse problems involving nonlinear partial differential equations," *Journal of Computational Physics*, vol. 378, pp. 686–707, 2019, doi: 10.1016/j.jcp.2018.10.045.

[46] S. Jaballah, G. Neri, H. Dahman, N. Donato, and L. E. Mir, "Development of a Ternary AlMgZnO-Based Conductometric Sensor for Carbon Oxides Sensing," *IEEE Transactions on Instrumentation and Measurement*, vol. 70, pp. 1–7, 2021, doi: 10.1109/tim.2021.3066169.

[47] W. Yan *et al*., "Conductometric gas sensing behavior of WS2 aerogel," *FlatChem*, vol. 5, pp. 1–8, 2017, doi: 10.1016/j.flatc.2017.08.003.

[48] Y. Kim, S. Goo, and J. S. Lim, "Multi-Gas Analyzer Based on Tunable Filter Non-Dispersive Infrared Sensor: Application to the Monitoring of Eco-Friendly Gas Insulated Switchgears," *Sensors*, vol. 22, no. 22, p. 8662, 2022, doi: 10.3390/s22228662.

[49] Z. Witkiewicz, K. Jasek, and M. Grabka, "Semiconductor Gas Sensors for Detecting Chemical Warfare Agents and Their Simulants," *Sensors*, vol. 23, no. 6, p. 3272, 2023, doi: 10.3390/s23063272.

[50] Y. Liang *et al*., "Field comparison of electrochemical gas sensor data correction algorithms for ambient air measurements," *Sensors and Actuators B: Chemical*, vol. 327, p. 128897, 2021, doi: 10.1016/j.snb.2020.128897.

[51] Q. Xu *et al*., "Comprehensive study of the low-temperature oxidation chemistry by synchrotron photoionization mass spectrometry and gas chromatography," *Combustion and Flame*, vol. 236, p. 111797, 2022, doi: 10.1016/j.combustflame.2021.111797.

[52] S. Golgiyaz, M. F. Talu, and C. Onat, "Artificial neural network regression model to predict flue gas temperature and emissions with the spectral norm of flame image," *Fuel*, vol. 255, p. 115827, 2019, doi: 10.1016/j.fuel.2019.115827.

[53] A. Mähler, T. Schütte, J. Steiniger, and M. Boschmann, "The Berlin-Buch respiration chamber for energy expenditure measurements," *European Journal of Applied Physiology*, vol. 123, no. 6, pp. 1359–1368, 2023, doi: 10.1007/s00421-023-05164-w.

[54] D. d'Hose, P. Danhier, H. Northshield, P. Isenborghs, B. F. Jordan, and B. Gallez, "A versatile EPR toolbox for the simultaneous measurement of oxygen consumption and superoxide production," *Redox Biology*, vol. 40, p. 101852, 2021, doi: 10.1016/j.redox.2020.101852.

[55] B. Fu *et al*., "Recent progress on laser absorption spectroscopy for determination of gaseous chemical species," *Applied Spectroscopy Reviews*, vol. 57, no. 2, pp. 112–152, 2020, doi: 10.1080/05704928.2020.1857258.

[56] M. Wieland, Y. Li, and S. Martinis, "Multi-sensor cloud and cloud shadow segmentation with a convolutional neural network," *Remote Sensing of Environment*, vol. 230, p. 111203, 2019, doi: 10.1016/j.rse.2019.05.022.

[57] A. Akhmadiya, N. Nabiyev, K. Moldamurat, K. Dyussekeyev, and S. Atanov, "Use of Sentinel-1 Dual Polarization Multi-Temporal Data with Gray Level Co-Occurrence Matrix Textural Parameters for Building Damage Assessment," *Pattern Recognition and Image Analysis*, vol. 31, no. 2, pp. 240–250, 2021, doi: 10.1134/s1054661821020036.

[58] A. E. Kyzyrkanov, S. K. Atanov, and S. Abdel Rahman Aljawarneh, "Formation control and coordination of swarm robotic systems," *The 7th International Conference on Engineering & MIS 2021*, pp. 1-11, 2021, doi: 10.1145/3492547.3492704.

[59] A. Kyzyrkanov, S. Atanov, and S. Aljawarneh, "Coordination of movement of multiagent robotic systems," *2021 16th International Conference on Electronics Computer and Computation (ICECCO)*, pp. 1-4, 2021, doi: 10.1109/ICECCO53203.2021.9663796.

[60] Z. Oralbekova, Z. Khassenova, B. Mynbayeva, M. Zhartybayeva, and K. Iskakov, "Information system for monitoring of urban air pollution by heavy metals," *Indonesian Journal of Electrical Engineering and Computer Science*, vol. 22, no. 3, p. 1590, 2021, doi: 10.11591/ijeecs.v22.i3.pp1590-1600.

[61] K. Laganovska *et al*., "Portable low-cost open-source wireless spectrophotometer for fast and reliable measurements," *HardwareX*, vol. 7, p. e00108, 2020, doi: 10.1016/j.ohx.2020.e00108.

[62] J. S. Botero-Valencia and J. Valencia-Aguirre, "Portable low-cost IoT hyperspectral acquisition device for indoor/outdoor applications," *HardwareX*, vol. 10, p. e00216, 2021, doi: 10.1016/j.ohx.2021.e00216.

[63] B. Sivakumar and C. Nanjundaswamy, "Weather monitoring and forecasting system using IoT," *Global Journal of Engineering and Technology Advances*, vol. 8, no. 2, pp. 008–016, 2021, doi: 10.30574/gjeta.2021.8.2.0109.

[64] E. J. Davis and B. H. Clowers, "Low-cost Arduino controlled dual-polarity high voltage power supply," *HardwareX*, vol. 13, p. e00382, 2023, doi: 10.1016/j.ohx.2022.e00382.

[65] Z. Mukanova, S. Atanov, and M. Jamshidi, "Features of Hardware and Software Smoothing of Experimental Data of Gas Sensors," *2021 IEEE International Conference on Smart Information Systems and Technologies (SIST)*, pp. 1-6, 2021, doi: 10.1109/SIST50301.2021.9465981.

[66] R. Y. Choi, A. S. Coyner, J. Kalpathy-Cramer, M. F. Chiang, and J. P. Campbell, "Introduction to machine learning, neural networks, and deep learning," *Translational vision science & technology*, vol. 9, no. 2, pp. 14-14, 2020.

[67] D. Adams, D.-H. Oh, D.-W. Kim, C.-H. Lee, and M. Oh, "Prediction of SOx–NOx emission from a coal-fired CFB power plant with machine learning: Plant data learned by deep neural network and least square support vector machine," *Journal of Cleaner Production*, vol. 270, p. 122310, 2020, doi: 10.1016/j.jclepro.2020.122310.

[68] G. Shen, D. Zhao, and Y. Zeng, "Backpropagation with biologically plausible spatiotemporal adjustment for training deep spiking neural networks," *Patterns*, vol. 3, no. 6, p. 100522, 2022, doi: 10.1016/j.patter.2022.100522.

[69] X. Niu, L. Shi, H. Wan, Z. Wang, Z. Shang, and Z. Li, "Dynamic functional connectivity among neuronal population during modulation of extra-classical receptive field in primary visual cortex," *Brain Research Bulletin*, vol. 117, pp. 45–53, 2015, doi: 10.1016/j.brainresbull.2015.07.003.

[70] Y. Wu, L. Deng, G. Li, J. Zhu, and L. Shi, "Spatio-Temporal Backpropagation for Training High-Performance Spiking Neural Networks," *Frontiers in Neuroscience*, vol. 12, 2018, doi: 10.3389/fnins.2018.00331.

[71] K. Beer *et al*., "Training deep quantum neural networks," *Nature Communications*, vol. 11, no. 1, 2020, doi: 10.1038/s41467-020-14454-2.

[72] G. Zaid, L. Bossuet, F. Dassance, A. Habrard, and A. Venelli, "Ranking Loss: Maximizing the Success Rate in Deep Learning Side-Channel Analysis," *IACR Transactions on Cryptographic Hardware and Embedded Systems*, pp. 25–55, 2020, doi: 10.46586/tches.v2021.i1.25-55.

[73] A. M. Mouazen, B. Kuang, J. D. Baerdemaeker, and H. Ramon, "Comparison among principal component, partial least squares and back propagation neural network analyses for accuracy of measurement of selected soil properties with visible and near infrared spectroscopy," *Geoderma*, vol. 158, no. 1–2, pp. 23–31, 2010, doi: 10.1016/j.geoderma.2010.03.001.

[74] J. Bilski, B. Kowalczyk, A. Marchlewska, and J. M. Zurada, "Local Levenberg-Marquardt Algorithm for Learning Feedforwad Neural Networks," *Journal of Artificial Intelligence and Soft Computing Research*, vol. 10, no. 4, pp. 299–316, 2020, doi: 10.2478/jaiscr-2020-0020.

[75] E. A. Muravyova and N. N. Uspenskaya, "Development of a Neural Network for a Boiler Unit Generating Water Vapour Control," *Optical Memory and Neural Networks*, vol. 27, no. 4, pp. 297–307, 2018, doi: 10.3103/s1060992x18040070.

[76] N. N. S. Torres, H. F. Scherer, O. H. Ando Junior, and J. J. G. Ledesma, "Application of Neural Networks in a Sodium-Nickel Chloride Battery Management System," *Journal of Control, Automation and Electrical Systems*, vol. 33, no. 4, pp. 1188–1197, 2022, doi: 10.1007/s40313-021-00847-1.

[77] V. S. Bawa and V. Kumar, "Linearized sigmoidal activation: A novel activation function with tractable non-linear characteristics to boost representation capability," *Expert Systems with Applications*, vol. 120, pp. 346–356, 2019, doi: 10.1016/j.eswa.2018.11.042.

[78] J. Feng and S. Lu, "Performance Analysis of Various Activation Functions in Artificial Neural Networks," *Journal of Physics: Conference Series*, vol. 1237, no. 2, p. 022030, 2019, doi: 10.1088/1742-6596/1237/2/022030.

[79] Z. A. Mukanova and S. K. Atanov, "Gas analyzer," Patent for a useful model No. 5141. Bulletin No. 27., Kazakhstan, 2020 [Муканова Ж.А., Атанов С.Б. «Газоанализатор» // Патент РК на полезную модель № 5141. 2020. Бюл. № 27].

[80] Z. A. Mukanova and S. K. Atanov, "Intelligent gas analyzer," Patent for a useful model No. 8288. Bulletin No. 29., Kazakhstan, 2023 [Муканова Ж.А., Атанов С.Б. «Интеллектуальный газоанализатор» // Патент РК на полезную модель № 8288. 2023. Бюл. № 29].